ACOUSTIC MODELING OF SPARK ARRESTOR FOR DIESEL ENGINES

M. M. Ammar[1], Tamer Elnady[2], Tarek Osman[3] and Waleed El-Sallamy[4]
[1]Department of Force and Material Metrology, National Institute of Standards, El Haram, Giza, Egypt
[2]Design and Production Engineering, Ain shams University, Ain Shams University, Elsarayat St., Abbaseya, Cairo, Egypt
[3]Department of Mechanical Design and Production, Cairo University, Gamaa Street, Giza, Egypt
[4]Department of Production Engineering and Printing Technology, Akhbar Elyom Academy, 4th Industrial Zone, 6th of October City, Giza, Egypt
E-Mail: eng.moh.ammar@gmail.com

ABSTRACT

Diesel engines emit sparks as a result of breaking and burning of carbon deposition inside engine cylinders and exhaust system. Spark Arrestor plays a critical role in impeding the embers emission as it arrests and traps the embers and the sparks inside it. The objective of this paper is to Design, Model, and Simulate Spark Arrestors in terms of Acoustic Performance. Two models of Spark Arrestors were selected; one Commercial and a newly developed centrifugal Spark Arrestor. The Acoustics design and Simulations were performed using two port theory where, the Spark Arrestor models are limited to the plane wave range. These models were implemented in SIDLAB software for simulating the propagation of low frequency Sound and air flow in Ducts. The theoretical modeling for the two models was shown to be matched with the experimental verification in terms of transmission loss within 92% to 98%, and in terms of pressure drop within 86% to 99%.

Keywords: spark arrestor, ember, TL, diesel **e**ngine, two-port theory.

1. INTRODUCTION

Business, economy, and life are affected extremely by fire and explosion. Sparks and embers which are emitted from Diesel Engines could lead to fire and explosion if they touched flammable materials[1]. These sparks are produced as a result of the incomplete reaction of the fuel which produces carbons that burnt as a result of the exhaust high flow rate and temperature. Spark Arrestors are used to trap these sparks and embers.

The necessity for Spark Arrestors was established with the introduction of wood burning locomotives in 1830, and they were first applied in the form of a wire netting cap placed over the top of the smokestack[2]. Later, the 20th century especially in 1964, the interest of noise reduction using Spark Arrestors were introduced by using absorption materials. The aim of this paper is to study the acoustic performance for two types of Spark Arrestors. Theoretical modeling and experimental verification were done to compare between a Centrifugal model of Diesel Engine spark arrestor and a commercial Spark Arrestor in terms of Sound Transmission Loss and pressure drop.

2. THEORETICAL BACKGROUND

There are four main methodologies that are used in arresting Sparks namely; Particles Impact, Refinery meshing, Electrostatic charge, Particles' Grinding, and Centrifugal Force. Where in Centrifugal Type Spark Arrestor, Stationary baffles are used to remove the ash or embers from the exhaust gas by centrifugal force. This paper focuses on Spark Arrestor Centrifugal Type acoustic performance sound transmission loss and its effect upon raised pressure drop.

2.1 Theoretical Modeling of Spark Arrestors' Flow Calculations

For the purpose of acoustic modeling, duct systems or networks are often too complicated to enable the direct solution of the governing equations. One method to describe the sound transmission along the system is called the building block method or two-port transfer matrix method[3]. This method splits the system into several smaller duct parts, acoustic elements, in which the sound propagation is well defined. Plane waves are assumed to propagate between different elements and the sound field can be characterized by two state variables. One convenient choice is to use acoustic pressure and volume velocity. The sound propagation inside each element is analyzed separately and higher order modes can exist inside the element. A 2x2 complex transfer matrix completely describes the sound transmission through each element. The pressure and volume velocity of each element at the inlet and outlet can be related to the following expression [4],[5].

$$\begin{bmatrix} p_1 \\ q_1 \end{bmatrix} = \begin{bmatrix} T_{11} & T_{12} \\ T_{21} & T_{22} \end{bmatrix} \begin{bmatrix} p_2 \\ q_2 \end{bmatrix} + \begin{bmatrix} p^s \\ q^s \end{bmatrix} \quad (1)$$

As q and p are the volume velocity and the pressure, 1 refers to the inlet and 2 refers to the outlet, T_{ij} is the element of the two-port transfer matrix, and the p_s and q_s are the source pressure and volume velocity.

$$\begin{bmatrix} P_1 \\ q_1 \end{bmatrix} = \begin{bmatrix} 1 & Z \\ 0 & 1 \end{bmatrix} \begin{bmatrix} P_2 \\ q_2 \end{bmatrix} \quad (2)$$

where Z is the lumped ('point wise') impedance associated with the two-port element, and is given by $Z = Z_w/S_w$ (where Z_w is the perforate acoustic impedance and S_w is the duct wall area of the perforated segment), and 1

ARPN Journal of Engineering and Applied Sciences

denotes the inlet side and 2 denotes the outlet side. Only plane waves are assumed to propagate on each side of the perforate, and parallel to the wall. The perforate impedance used in this work is calculated according to reference[3].

The SIDLAB software[4] used in this work is based on the representation of a duct network as a network of two-ports. The two-port elements are then joined and analyzed using the method described in reference[6].SIDLAB couples the elements at each node, using the continuity of pressure and volume velocity.

2.2 Theoretical Modeling of Spark Arrestors' Flow Calculation

In order to include the pressure drop related to the investigated duct systems, this property needs to be modeled. For the flow modeling applied in this work, the same SIDLAB algorithm [7] used to calculate the sound propagation can in principle be used to calculate the pressure drop. Each two-port element can be described by a flow transfer matrix to relate the stagnation pressure and volume flow. Unlike the acoustic calculations, the flow calculation is only performed at one "frequency". The flow two-ports can be described by

$$\begin{bmatrix} P_1 \\ Q_1 \end{bmatrix} = \begin{bmatrix} 1 & R_f \\ 0 & 1 \end{bmatrix} \begin{bmatrix} P_2 \\ Q_2 \end{bmatrix} \quad (3)$$

where P is the stagnation pressure, Q is the volume flow and incompressible flow is assumed. It is important to calculate the flow resistance, R_f, for each two-port in the network. In fluid flow handbooks, one can find the head loss or loss coefficient k_e across any element. The loss coefficient is a constant which depends on the geometry of the element. The flow resistance is related to the loss coefficient by

$$R_f(Q) = k_e \frac{\rho}{2S^2} |Q| \quad (4)$$

Where S is the cross-sectional area of the inlet section and ρ is the density (constant).

3. DESIGN AND MODELING

This part shows the configurations and the work theory for the commercial Spark Arrestor and the new developed Spark Arrestor.

3.1 Commercial Spark Arrestor of Centrifugal Collection Type

Commercial spark arrestor (Figure-1 and Figure-2) is of centrifugal collection type according to standard BS EN 1834-3:2000 [8].

Accordingly particles will pass through three chambers except for part of these particles will stay outside the Spark Arrestor as a result of the inlet deflection blades. As most of the particles will be trapped in the second and third chambers due to the centrifugal force that affects particles. This centrifugal force is as a result of exhaust gas rotation due to the inclined blades fixed at each slot opening of the Spark Arrestor part ends, seeFigure-1. Also, part of the particles which succeed in reaching the outlet will be impeded by the outlet deflection blades.

This Spark Arrestor consists of inlet pipe 50.8 mm, two inlet deflection blades, expansion chamber of diameter 152.4 mm and of length 445.5 mm, two internal plates with middle hole of 116.7 mm, two outlet deflection blades, outlet pipe 50.8 mm, and Spark Arrestor part which consists of pipe of diameter 115 mm and length 360 mm. This Spark Arrestor part is closed by a plug at its outlet end. It has slots with inclined blades of length 80 mm and opening height 2 mm which are distributed around the Spark Arrestor circumference at its two ends which cause the exhaust gas to be rotated. Also, at the middle of its length, it has slots of length 47 mm and of height 2 mm.

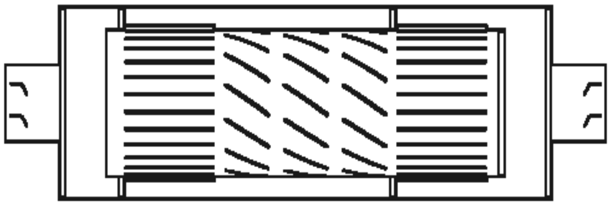

Figure-1. Schematic drawing of commercial Spark arrestor.

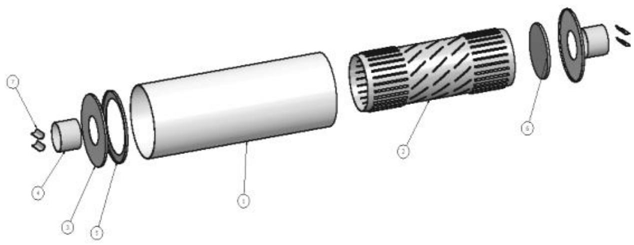

Figure-2. Commercial Spark arrestor sub assembly.

3.2 Centrifugal Collection Spark Arrestor Type

The newly developed Spark Arrestor [9](Figure-3 and Figure-4) is of centrifugal collection type according to standard BS EN 1834-3:2000[8]. Particles will pass to the first chamber which will be affected by the centrifugal force as a result of flow rotation due to the inclined blades which are fixed at each slot opening of the Spark Arrestor part. Then these particles will be trapped before passing to the second chamber as a result of particles weight and the perforated plate no. 2, see Figure-3 and Figure-4.

This new developed Spark Arrestor consists of inlet pipe 76.2 mm of length 75 mm, Expansion chamber of diameter 200 mm and length 300 mm, Internal perforated plate, Outlet pipe of 76.2 mm, and Spark Arrestor part, part no. 7, of ten ribs and each rib contains a slot of 2 mm height and 160 mm length. Each slot has a blade that causes the exhaust gas to be rotated.

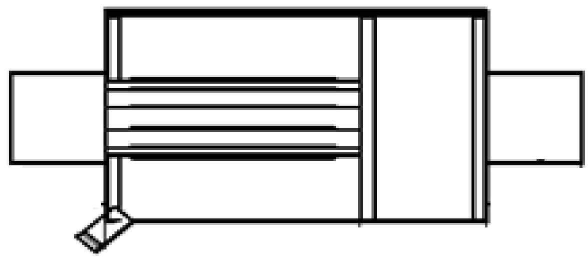

Figure-3. Schematic drawing of Spark arrestor.

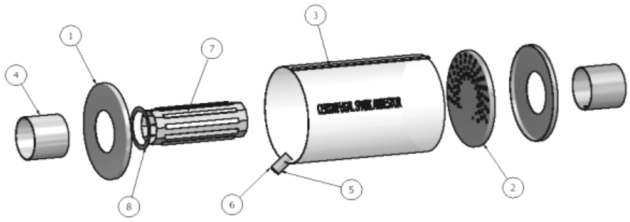

Figure-4. Newly developed Spark arrestor subassembly.

3.3 Theoretical Modeling of Spark Arrestors' Sound Transmission Loss

SIDLAB is used in simulating the sound in ducts as mentioned before. In this study, the SIDLAB is used to simulate the sound TL of the new developed Spark Arrestor and the commercial Spark Arrestor. As in SIDLAB, each Spark Arrestor is classified into several parts with a certain arrangement referred to as, network. Each part dimensions in this network shall be indicated. The inlet and outlet points of the network shall also be indicated to specify the air flow direction. In the following part, the two networks for the two Spark Arrestors will be shown.

3.3.1 Commercial Spark Arrestor

The Commercial Spark Arrestor contains two-port elements and four-port elements, as shown inFigure-5, as each two-port element connected to two nodes, one at the inlet and the other at the outlet. While the two-port elements can affect the system by 4 nodes in which they are 2 inlets and 2 outlets but, in this case, the four-port element affect the network by one node at the inlet and one node at the outlet.

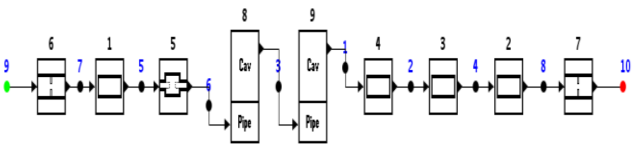

Figure-5. SIDLAB network for the Commercial Spark Arrestor.

3.3.2 The new developed Spark Arrestor

The New Developed Spark Arrestor Spark Arrestor contains two-port elements only, as shown in Figure-6, as each element connected to two nodes, one at the inlet and the other at the outlet.

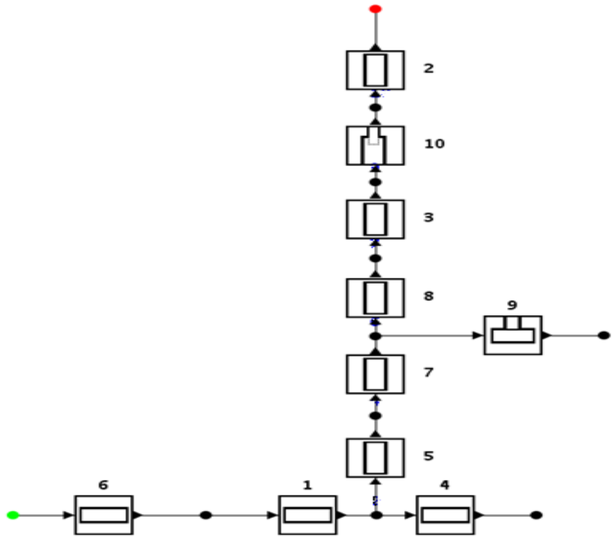

Figure-6. SIDLAB network for the newly developed Spark Arrestor.

3.4 Theoretical Modeling of Spark Arrestors' Pressure Drop

This part shows the pressure drop theoretical modeling in SIDLAB for the new model of the Spark Arrestor and the commercial Spark Arrestor using the same network of the sound TL simulation in SIDLAB (Figure-5 and Figure-6). The same theory is used in calculating the pressure drop and the sound TL which is the two-port theory as mentioned before.

4. EXPERIMENTAL WORK

The method which is used in measuring the sound TL of Spark Arrestors is the two-source method. It is based on the transfer matrix. The acoustical element can be modeled using its four-pole parameters, as shown in

Figure-7. The transfer matrix is

$$\begin{bmatrix}p_1\\q_1\end{bmatrix}=\begin{bmatrix}A & B\\C & D\end{bmatrix}\begin{bmatrix}p_2\\q_2\end{bmatrix} (5)$$

where p_1 and q_1 are the sound pressure amplitude and the volumetric velocity amplitude at the inlet. Also,p_2 and q_2 are the sound pressure amplitude and the volumetric velocity amplitude at the outlet, and A,B,C and D are the four pole parameters of the system.

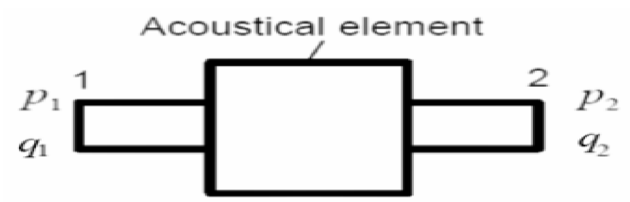

Figure-7. The Pipe four poles.

When the two-source method is used, two sound sources shall be used as shown inFigure-10. One sound source is installed at the spark arrestor inlet side and another sound source is installed at the spark arrestor

ISSN 1819-6608
ARPN Journal of Engineering and Applied Sciences

outlet side. The sound source at the inlet side will be used first in the experiment using transfer matrix method, so two equations only can be obtained, but there are four unknowns in which they are the four poles, A, B, C, and D, so the sound source at the other end will be used. Two other equations can be obtained then the four poles can be evaluated.

Then the Sound TL can be expressed in the terms of the four poles parameters and the tube areas as

$$TL = 20\log_{10}\{\tfrac{1}{2}\left|A_{23} + \frac{B_{23}}{\rho c} + \rho c.C_{23} + D_{23}\right|\} + 10\log_{10}\left(\frac{S_i}{S_o}\right) \quad (6)$$

The Sound TL test rig was built according to ISO 10534-2: 1998 [10].

In this paper, two test rigs were used; one is used to measure the sound TL of the new developed Spark Arrestor, as shown inFigure-8, and the other test rig is used to measure also the sound TL of the Commercial Spark Arrestor, as shown in Figure-9.

The first test rig inner diameter is 50 mm and is made of stainless steel while the second test rig inner diameter is 25 mm and is made of Aluminum.

Figure-8. New developed Spark Arrestor sound TL test rig.

Figure-9. Commercial model sound TL test rig.

Loudspeakers are mounted at equal distances at both sides upstream and downstream. Six microphones are flush mounted in the tube wall as the three upstream microphones and the three downstream microphones are used to cover the plane waves range only in the test duct.
For the first test rig, Figure-8, the distance between the microphones of low frequency is 0.32 m, while the distance between the microphones of high frequency is 0.04 m. The distance between the test object and the closest microphone is 0.55 m at the upstream side and 0.564 m at the downstream side for the newly developed Spark Arrestor.

For the second test rig, Figure-9, the distance between the microphones of low frequency is 0.24 m, while the distance between the microphones of high frequency is 0.03 m. The distance between the test object and the closest microphone is 0.151 m.

The measurement system consists of six microphones which are connected with Amplifier; two mufflers are connected at the ends of the test rig to prevent the wave reflections. Signals from the loudspeakers and the microphones are fed into the data acquisition system as input and output signals. The loudspeakers signal is used as the reference signal. The input and output signals are converted by Lab View data acquisition software system into digital signals and then processed by SIDLAB to calculate the sound TL using the two-source method. The microphones are then calibrated using the first microphone as the reference microphone. The measurement for the upstream direction is done one time, and then for the downstream direction also one time. The loudspeaker is started from 30 Hz as it doesn't give good response below this frequency.

The pressure drop was measured across the Spark Arrestors using a digital manometer.

The measurement systems of both TL and pressure drop are illustrated in Figure-10and Figure-11 respectively.

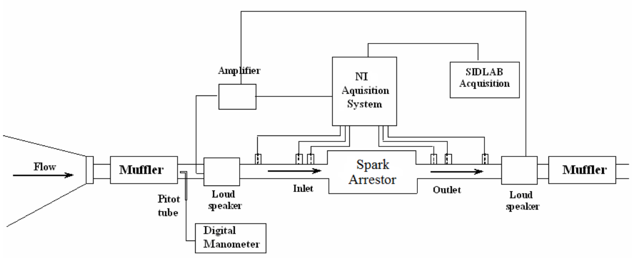

Figure-10. Schematic for sound TL measuring system.

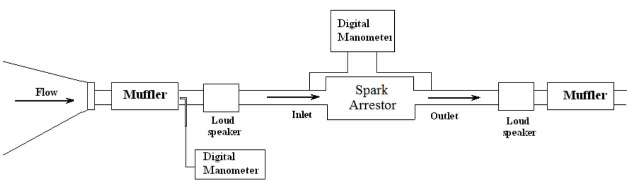

Figure-11. Schematic for pressure drop measuring system.

5. RESULTS

This part shows the theoretical and the experimental results for the Spark Arrestors' transmission loss, pressure drop and their simulation error.

5.1 Commercial Spark Arrestor

This part shows the correlation between the theoretical modeling results and the Experiment results of the Commercial Spark Arrestor.

VOL. 16, NO. 3, FEBRUARY 2021 ISSN 1819-6608
ARPN Journal of Engineering and Applied Sciences

www.arpnjournals.com

5.1.1 Spark Arrestor sound TL

The simulation mean error difference is about 18.14% for the Sound TL without flow as shown in Figure-12, and about -11.26% for Sound TL at flow speed 4m/s as shown in Figure-13, and about -29.5% for Sound TL at flow speed 7m/s as shown in Figure-14, and about -45% for Sound TL at flow speed 10 m/s as shown in Figure-15.

These simulations mean errors result from the uncertainty in the measurement tools used in measuring the dimensions of the Spark Arrestor real model after its manufacturing. Also, the modifications which were done in the Spark Arrestor model (the number of louvers were reduced from 26x2 slots to 13x2 slots, and their areas are increased after the reduction of the slots' number), these modifications were done for software adaptation.

This also happened due to the existence of the plug at the outlet of the Spark Arrestor part, as the three-dimensional effects appear.

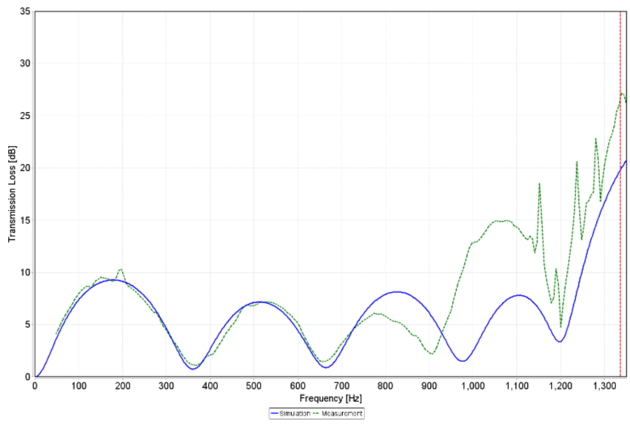

Figure-12. Sound TL experimental and theoretical results without flow.

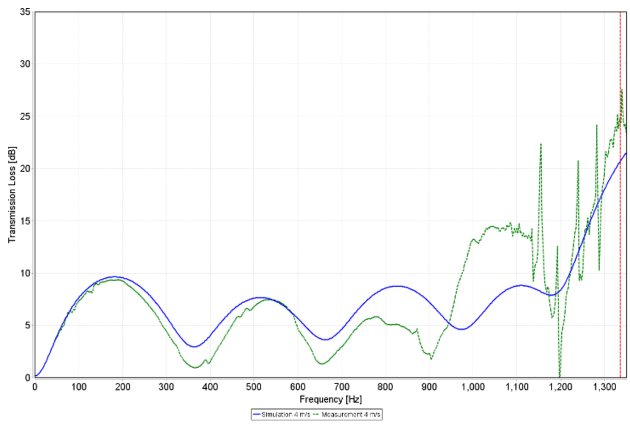

Figure-13. Sound TL experimental and theoretical results with 4 m/s flow speed.

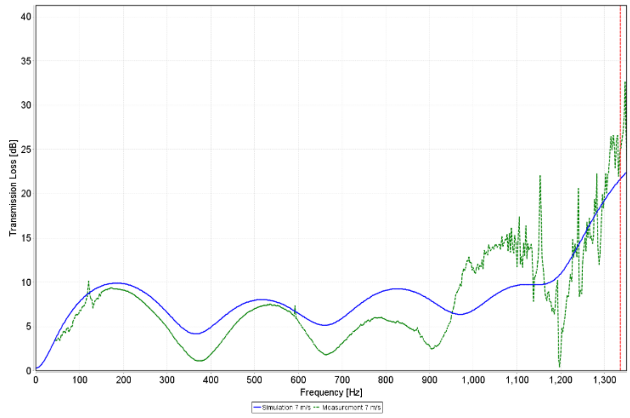

Figure-14. Sound TL experimental and theoretical results with 7 m/s flow speed.

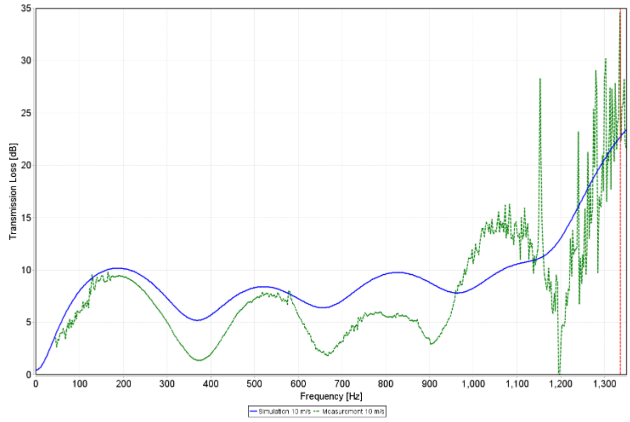

Figure-15. Sound TL experimental and theoretical results with 10 m/s flow speed.

In general, the agreement between the simulated and the measured results was quite good up to frequency 840 Hz before the appearance of the three-dimensional effects except at flow speed 10 m/s was quite fair. Also, the agreement between peaks locations and amplitudes is good up to frequency 840 Hz before the appearance of the three-dimensional effects.

5.1.2 Spark Arrestor pressure drop

The Experimental Pressure Drop function of flow speed is $\Delta P = 7.427v^2 + 3.088v - 2.581$ with an average error 0.012%. The simulation mean error is about -10%, as shown in Figure-16. This error due to the modifications which were done to the Spark Arrestor part as previously mentioned in the collection efficiency of the same model.

VOL. 16, NO. 3, FEBRUARY 2021 ISSN 1819-6608
ARPN Journal of Engineering and Applied Sciences

www.arpnjournals.com

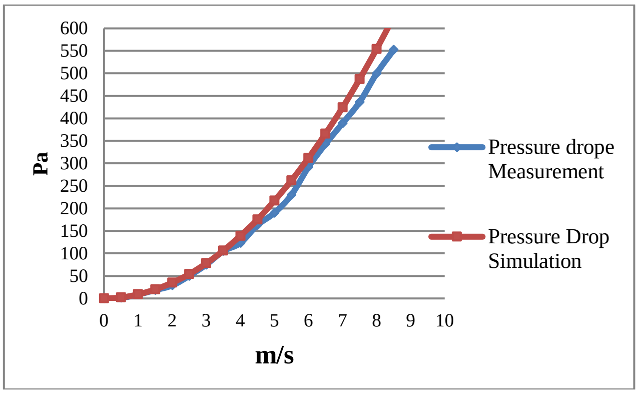

Figure-16. Pressure drop.

5.2 The New Developed Spark Arrestor

This part shows the correlation between the theoretical modeling results and the Experiment results of the new developed Spark Arrestor.

5.2.1 Spark Arrestor sound TL

The simulation mean error is about 35% for the Sound TL without flow as shown in Figure-17, and about 20% for the Sound TL with flow speed 10m/s as shown inFigure-18, and about 28% for the Sound TL with flow speed 25m/s as shown inFigure-19, and finally about 35 % for the Sound TL with flow speed 40m/s as shown inFigure-20.

These simulations mean errors result from the modifications that happen in the Spark Arrestor model in SIDLAB by assuming that the slots opening in the Spark Arrestor part are perforations and assuming that its polygonal body is a cylindrical body. While, in case of without flow, in addition to the previous reasons, the simulation mean error happens due to the existence of the plug at the outlet of the Spark Arrestor part, as the three-dimensional effects appear.

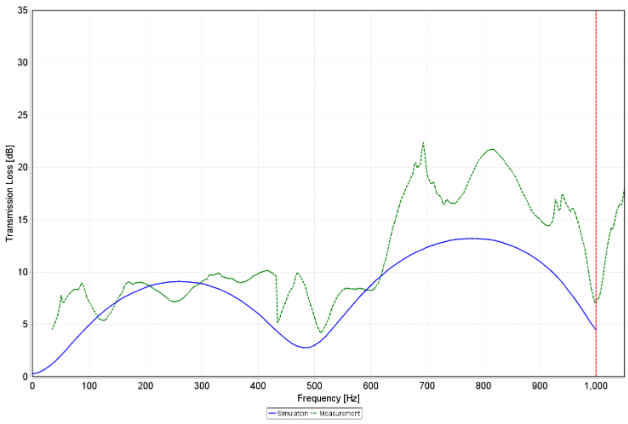

Figure-17. Sound TL experimental versus theoretical results without flow.

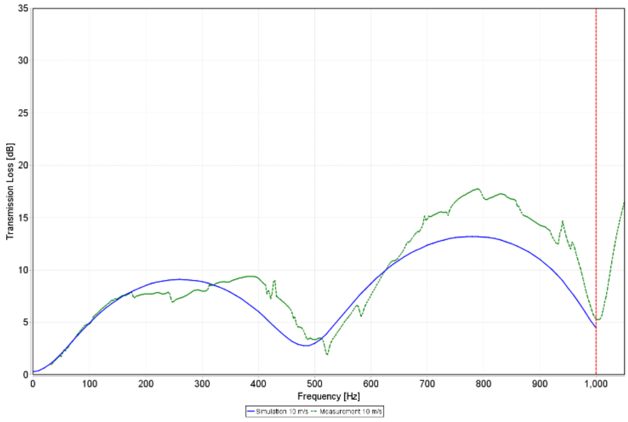

Figure-18. Sound TL experimental and theoretical results with 10 m/s flow speed.

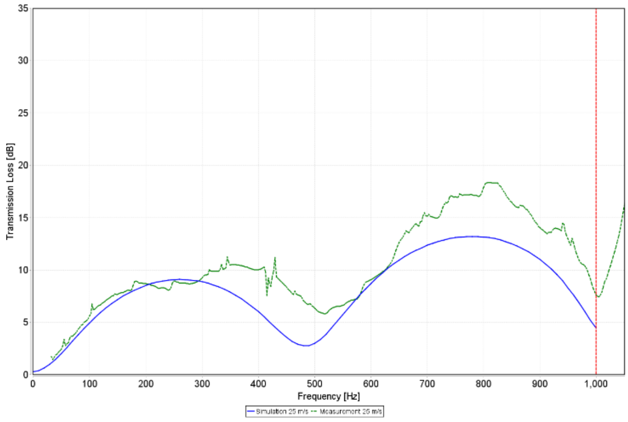

Figure-19. Sound TL experimental and theoretical results with 25 m/s flow speed.

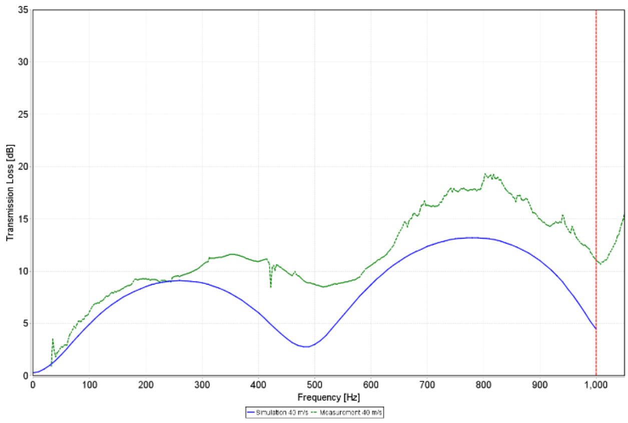

Figure-20. Sound TL experimental and theoretical results with 40 m/s flow speed.

In general the agreement between the simulated and the measured results until the cut-off frequency of the first mode of the connecting elements was quite fair in cases of no flow speed and 40 m/s flow speed, but quite good in cases of 10 m/s and 25 m/s flow speeds. The agreement between peaks locations and amplitudes in all cases are good.

VOL. 16, NO. 3, FEBRUARY 2021 ISSN 1819-6608
ARPN Journal of Engineering and Applied Sciences

www.arpnjournals.com

5.2.2 Spark Arrestor pressure drop

The Experimental Pressure Drop function of flow speed is $\Delta P= 0.631v^2 - 0.727v + 8.303$ with an average error of about 0.0085%. This equation can be used to assume the pressure drop of Spark Arrestor at any flow speed. The simulation mean error is -1.73%, as shown in Figure-21, due to the modifications which were done in the Spark Arrestor model in SIDLAB which are assuming the slots openings in the Spark Arrestor part as perforations and assuming its polygonal body as a cylindrical body.

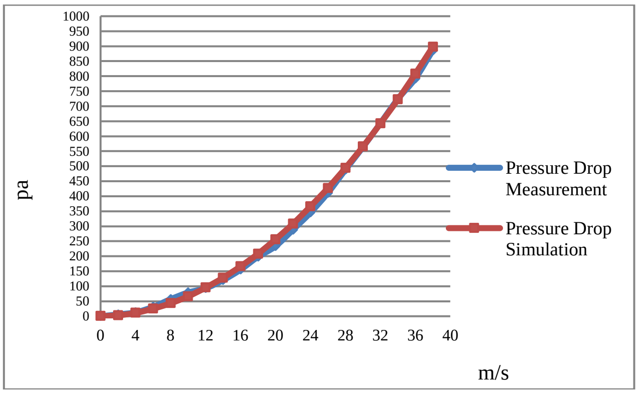

Figure-21. Pressure drop.

5.3 Performance Comparison

A comparison was done theoretically and experimentally between the newly developed model of Spark Arrestor and the commercial one.

The sound transmission loss is used for determining the Spark Arrestors performance. As shown in Figure-22and Figure-23 for the sound TL measurements, the new model of Spark Arrestor shows more sound TL than the commercial one.

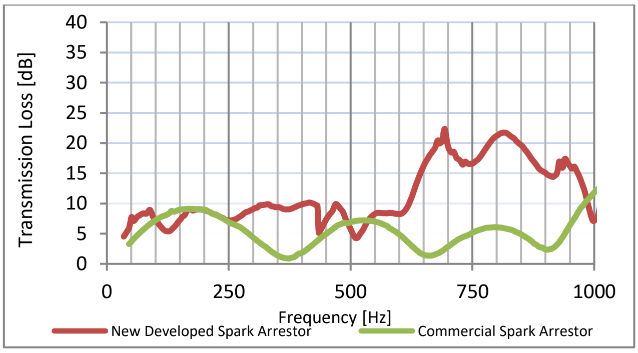

Figure-22. TL comparison at flow speed 0 m/s.

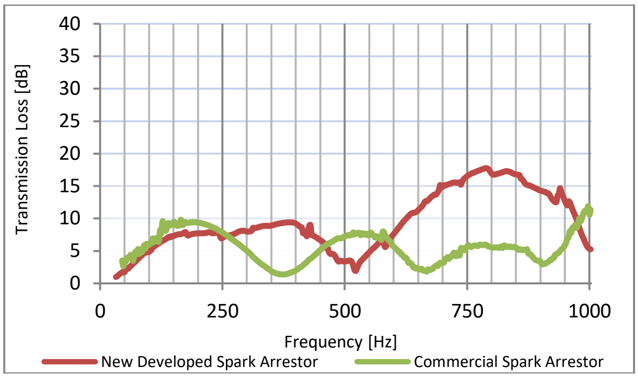

Figure-23. TL comparison at Flow Speed 10 m/s.

The pressure drop measurement is important in case of internal combustion engines, as high back pressure has a negative effect on engine efficiency resulting in a decrease of power output that must be compensated by increasing fuel consumption. In this study as shown in Figure-24, the new model of Spark Arrestor was shown to have considerably lower back pressure than the commercial one.

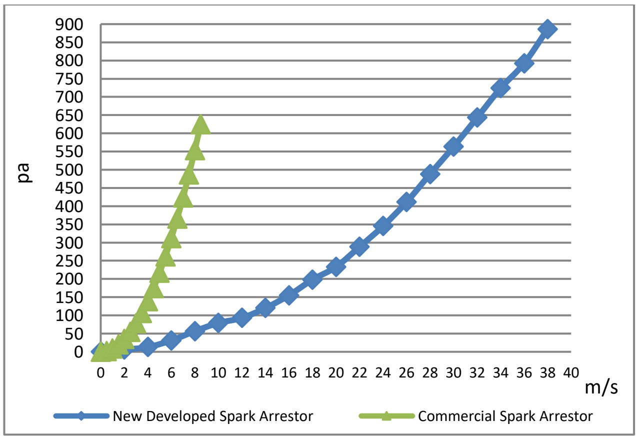

Figure-24. Comparison between Spark Arrestors' pressure drop measurement.

The production cost of the new developed Spark Arrestor is lower than the commercial one by 5.1% of its cost. Therefore, based on the previous results, the new developed Spark Arrestor is shown to have a considerable advantage than the commercial one.

6. CONCLUSIONS

The Spark Arrestor is a device which traps the exhaust carbon particles. In this paper, simulation technique was used in studying Spark Arrestors in terms of sound transmission loss (TL), and pressure drop using a new developed model of Spark Arrestors and a commercial one. Then this simulation results were compared with the Experimental results.

The theoretical modeling for the Spark Arrestors was shown to be matched with the experimental verification in terms of transmission loss within 92% to 98%, and in terms of pressure drop within 86% to 99%.

The sound transmission loss is used for determining the Spark Arrestors acoustic performance. As shown in the previously the sound TL measurements of the new model of Spark Arrestor show higher sound TL than the commercial one.

The pressure drop measurement is an important parameter for internal combustion engines, in this work, the new Spark Arrestors show lower back pressure than the commercial one.

The cost of the new Spark Arrestor is lower than the commercial one by 5.1% than the commercial Spark Arrestor.

So, designing and modeling of Spark Arrestors before their manufacturing gives confidence in their overall Efficiency after their manufacturing which subsequently reduces their final product cost and manufacturing time.

REFERENCES

[1] D. Nolan. 1996. Handbook of Fire and Explosion Protection Engineering Principles, Second Edi. New Jersey, Noyes Publishing Co.

[2] F. Brewster. 1919. Locomotive spark-arrester.

[3] T. Elnady. 2004. Modelling and characterization of Perforates in Lined Ducts and Mufflers. Thesis, no. September, pp. 1-40, [Online]. Available: http://www.diva-portal.org/smash/record.jsf?pid=diva2:9676.

[4] T. Elnady and M. Åbom. 2006. SIDLAB: new 1D sound propagation simulation software for complex duct networks. in 13th International Congress on Sound and Vibration, pp. 2-6, [Online]. Available: https://www.researchgate.net/publication/293093826_SIDLAB_New_1D_sound_propagation_simulation_software_for_complex_duct_networks.

[5] M. Wagih, T. Elnady and M. Åbom. 2013. Analysis of duct networks at high frequencies using two-ports. INTER-NOISE NOISE-CON Congr. Conf. Proceedings, InterNoise13, pp. 6067-6076(10), [Online]. Available: http://www.ingentaconnect.com/contentone/ince/incecp/2013/00000247/00000001/art00020.

[6] R. Glav and M. Åbom. 1997. A General Formalism for Analyzing Acoustic 2-Port Networks. J. Sound Vib. 202(5): 739-747, doi: 10.1006/jsvi.1996.0808.

[7] T. Elnady, S. Elsaadany, and M. Åbom. 2011. Flow and Pressure Drop Calculation Using Two-Ports. J. Vib. Acoust. 133(4): 8,doi: 10.1115/1.4003593.

[8] BS EN 1834-3:2000 Reciprocating internal combustion engines. Safety requirements for design and construction of engines for use in potentially explosive atmospheres Group II engines for use in flammable dust atmospheres. .

[9] M. Ammar, W. Elsallamy, T. Elnady, and T. Osman. 2020. Design Development for Centrifugal Diesel Particulate Arrestor. (Under Review)ARPN Journal Eng. Appl. Sci.

[10] ISO 10534-2:1998 Acoustics - Determination of sound absorption coefficient and impedance in impedance tubes - Part 2: Transfer-function method, 1st ed. ISO Standards.